Optimum Element Lengths for Yagi–Uda Arrays

C. A. CHEN AND DAVID K. CHENG, FELLOW, IEEE

Abstract—**An analytical method is developed for the maximization of the directivity of a Yagi–Uda array by adjusting the lengths of the dipole elements. The effects of a finite dipole radius and the mutual coupling between the elements are taken into consideration. Currents in the array elements are approximated by three-term expansions with complex coefficients that convert the governing integral equations into matrix equations. Array directivity is maximized by a perturbation procedure that adjusts the lengths of all array elements simultaneously and that converges very rapidly. This method can be combined with the previously developed spacing-perturbation method to form a double-perturbation procedure and obtain a Yagi–Uda array of nonuniformly spaced elements of unequal lengths, which yields a maximum directivity.**

I. INTRODUCTION

IN A PREVIOUS paper [1] a method was presented for the maximization of the directivity of a Yagi–Uda array by adjusting the interelement spacings in a systematic manner. The effects of a finite dipole radius and the mutual coupling between the array elements were taken into consideration. A three-term expansion with complex coefficients was used to approximate the current distribution in the elements and to convert the governing integral equations into simultaneous algebraic equations. This approach has the advantage of rapid convergence in the numerical solution. For an array with N elements the largest matrices encountered are of a dimension $2N \times 2N$.

The method employed a spacing perturbation technique and was based upon a theorem [2], [3], which assured that the directivity of an array would be increased by a proper set of spacing adjustments. It was found [1] that, in a typical case, the directivity of a space-optimized 6-element Yagi–Uda array could be increased by more than 57 percent over that of an array with equally spaced directors. The radiation pattern for the optimized array was also found to have lower sidelobes and a slightly narrower main beam, in addition to having an increased field intensity in the direction of maximum radiation, as compared with that for the array with equally spaced directors.

Besides the interelement spacings, the lengths of the array elements present themselves as another set of parameters that could be adjusted for directivity increases. The problem first appeared to be a rather difficult one since the various element lengths come into play not only in distance expressions (as do the element spacings), but also in the limits of definite integrals. Ehrenspeck and Poehler [4] obtained some experimental results showing the dependence of the gain of Yagi–Uda arrays on director height for given director spacings and array lengths. Using the classical dipole theory of sinusoidal current distributions, Green [5] compiled an extensive collection of data listing maximum obtainable directivities for Yagi–Uda arrays of equally spaced elements. The lengths of the reflector, the driver, and the director elements (all director elements were of equal length) that combined to yield a maximum directivity were tabulated. As far as the authors can determine, no work has been reported in the literature that enables the systematic determination of the (unequal) element lengths of a Yagi–Uda array for directivity optimization

This paper employs a perturbation technique for determining the element lengths needed for directivity maximization, similar to that used for obtaining optimum element spacings [1]. The three-term theory developed by King and his associates [6] is used for finding the currents in the dipoles. The technique can be applied to an array with arbitrary spacings. Typical numerical results for a uniformly spaced array with optimum element lengths are presented, and radiation patterns and current distributions on the elements are plotted.

By combining the method developed in this paper with that in the previous paper [1], a double perturbation procedure is obtained that will yield optimum element spacings as well as optimum dipole lengths. The result is a Yagi–Uda array of nonuniformly spaced elements of different lengths with a maximum directivity for a given number of dipoles of a specified radius. Typical results of this double perturbation procedure are also presented. In order to bring out the essential steps of this development without being overly burdened by complicated mathematical expressions, much detailed work will be omitted and the reader will be referred to related earlier work.

II. CURRENT DISTRIBUTIONS IN YAGI–UDA ARRAY

Fig. 1 shows the sketch of a typical Yagi–Uda array of dipole elements, of which only the second one is driven by a source and all others are parasitic. Element 1 is a reflector and elements 3 to N are directors. The integral-equation formulation for the currents in the N elements using a three-term approximation for the driven element and two terms for the parasitic elements has been discussed before [1], [6]; only the more essential results

Manuscript received March 26, 1974; revised July 16, 1974.
The authors are with the Department of Electrical and Computer Engineering, Syracuse University, Syracuse, N. Y. 13210.

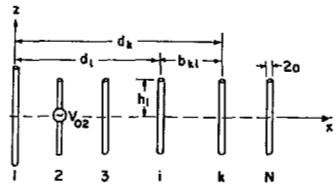

Fig. 1. Typical Yagi–Uda array.

will be included here. The N simultaneous integral equations to be solved are

$$\sum_{i=1}^{N} \int_{-h_i}^{h_i} I_i(z_i') K_{kid}(z_k,z_i')\, dz_i'$$

$$= \frac{j}{30 \cos \beta_0 h_k} [\tfrac{1}{2} V_{0k} \sin \beta_0(h_k - |z_k|) + U_k (\cos \beta_0 z_k - \cos \beta_0 h_k)], \qquad k = 1,2,\cdots,N \tag{1}$$

where β_0 is the phase constant, $V_{0k} = 0$, for $k \neq 2$, V_{02} is the excitation voltage of a δ-function generator in element 2

$$U_k = -j30 \sum_{i=1}^{N} \int_{-h_i}^{h_i} I_i(z_i') K_{ki}(h_k,z_i')\, dz_i' \tag{2}$$

$$K_{kid}(z_k,z_i') = K_{ki}(z_k,z_i') - K_{ki}(h_k,z_i')$$

$$= \frac{\exp[-j\beta_0 R_{ki}(z_k)]}{R_{ki}(z_k)} - \frac{\exp[-j\beta_0 R_{ki}(h_k)]}{R_{ki}(h_k)} \tag{3}$$

$$R_{ki}(z_k) = [(z_k - z_i')^2 + b_{ki}^2]^{1/2} \tag{4}$$

$$R_{ki}(h_k) = [(h_k - z_i')^2 + b_{ki}^2]^{1/2} \tag{5}$$

$$b_{kk} = a. \tag{6}$$

In solving the simultaneous integral equations (1), the current distributions $I_i(z)$ are assumed to have the following form:

$$I_i(z) = \sum_{m=1}^{3} A_i^{(m)} S_i^{(m)}(z) \tag{7}$$

with

$$S_i^{(1)}(z) = \sin \beta_0(h_i - |z|) \tag{8}$$

$$S_i^{(2)}(z) = \cos \beta_0 z - \cos \beta_0 h_i \tag{9}$$

$$S_i^{(3)}(z) = \cos \tfrac{1}{2}\beta_0 z - \cos \tfrac{1}{2}\beta_0 h_i \tag{10}$$

and $A_i^{(1)} = 0$, for $i \neq 2$. Substitution of (7) in (1) and use of certain approximate relations for the integrals involved yield

$$A_2^{(1)} = \frac{jV_{02}}{60\Psi_{22d}^{(1)} \cos \beta_0 h_2} \tag{11}$$

and two simultaneous matrix equations for the column matrices of complex coefficients $\{A^{(2)}\}$ and $\{A^{(3)}\}$:

$$[\Phi^{(2)}]\{A^{(2)}\} + [\Phi^{(3)}]\{A^{(3)}\} = -\{\Phi_2^{(1)}\} A_2^{(1)} \tag{12}$$

$$[\Psi_d^{(2)}]\{A^{(2)}\} + [\Psi_d^{(3)}]\{A^{(3)}\} = -\{\Psi_{2d}^{(1)}\} A_2^{(1)}. \tag{13}$$

The expressions for $\Psi_{22d}^{(1)}$ and for the elements of the $N \times N$ square matrices $[\Phi^{(2)}]$, $[\Phi^{(3)}]$, $[\Psi^{(2)}]$, and $[\Psi_d^{(3)}]$ as well as those for the elements of the $N \times 1$ column matrices $\{\Phi_2^{(1)}\}$ and $\{\Phi_{2d}^{(1)}\}$ are rather involved. They can be found in [6] and [7]. Suffice it to say that when the geometrical dimensions are given, the complex coefficients $A_2^{(1)}$, $\{A^{(2)}\}$, and $\{A^{(3)}\}$ can be determined from (11)–(13). With these coefficients known, the current distributions in all the dipole elements of a Yagi–Uda array can be obtained from (7). We note that the mutual coupling effects among the array elements are taken into consideration inherently in the formulation and that the currents in the elements can deviate much from a sinusoid [6], [7].

When the driven element (element 2) is a half-wave dipole, some of the quantities in the preceding formulation will become indeterminate and an alternative formulation is available [1], [7] in order to avoid computational difficulties. However, computational and experimental evidence [4], [5] indicates that none of the array elements will be very close to a half-wavelength in length in a maximum-directivity arrangement. Hence there will be no need to consider this special case. This conclusion is supported by the results of the numerical examples in Section VI.

III. LENGTH PERTURBATION

To adjust the element lengths in a Yagi–Uda array for maximum directivity it is assumed that the length of the ith element be changed by a small amount $\Delta h_i (\beta_0 \Delta h_i \ll 1)$. The perturbed currents $I_i^p(z)$ will be obtained from a modified version of (7):

$$I_i^p(z) = \sum_{m=1}^{3} A_i^{(m)p} S_i^{(m)p}(z) \tag{14}$$

with

$$S_i^{(1)p}(z) = \sin \beta_0(h_i + \Delta h_i - |z|) \cong S_i^{(1)}(z) + (\beta_0 \Delta h_i) \Delta S_i^{(1)}(z) \tag{15}$$

$$S_i^{(2)p}(z) = \cos \beta_0 z - \cos \beta_0(h_i + \Delta h_i) \cong S_i^{(2)}(z) + (\beta_0 \Delta h_i) \Delta S_i^{(2)}(z) \tag{16}$$

$$S_i^{(3)p}(z) = \cos \tfrac{1}{2}\beta_0 z - \cos \tfrac{1}{2}\beta_0(h_i + \Delta h_i) \cong S_i^{(3)}(z) + (\beta_0 \Delta h_i) \Delta S_i^{(3)}(z) \tag{17}$$

where

$$\Delta S_i^{(1)}(z) = \cos \beta_0(h_i - |z|) \tag{18}$$

$$\Delta S_i^{(2)}(z) = \sin \beta_0 h_i \tag{19}$$

$$\Delta S_i^{(3)}(z) = \tfrac{1}{2} \sin \tfrac{1}{2}\beta_0 h_i. \tag{20}$$

A similar approximation can be applied to the distance terms $R_{ki}(h_k)$ in (3) and (5), to account for the change Δh_k [8]. Perturbed definite integrals with element length

in the limits such as those in (1) and (2) may be written as follows:

$$\int_{-(h_i+\Delta h_i)}^{(h_i+\Delta h_i)} f(x)\,dx \cong \int_{-h_i}^{h_i} f(x)\,dx + \Delta h_i[f(h_i) - f(-h_i)]. \tag{21}$$

With these approximations and the substitution of the perturbed currents $I_i^p(z)$ in (1), the matrices $[\Phi^{(m)}]$, $[\Psi_d{}^{(m)}]$, $\{\Phi_2{}^{(1)}\}$, and $\{\Psi_{2d}{}^{(1)}\}$ and the complex coefficients $A_2{}^{(1)}$ and $\{A^{(m)}\}$ in (12) and (13) are changed to $[\Phi^{(m)}]^p$, $[\Psi_d{}^{(m)}]^p$, $\{\Phi_2{}^{(1)}\}^p$, $\{\Psi_{2d}{}^{(1)}\}^p$, $A_2{}^{(1)p}$, and $\{A^{(m)}\}^p$, respectively. We have

$$[\Phi^{(m)}]^p = [\Phi^{(m)}] + [\Delta\Phi^{(m)}], \qquad m = 2,3 \tag{22}$$

$$[\Psi_d{}^{(m)}]^p = [\Psi_d{}^{(m)}] + [\Delta\Psi_d{}^{(m)}], \qquad m = 2,3 \tag{23}$$

$$\{\Phi_2{}^{(1)}\}^p = \{\Phi_2{}^{(1)}\} + \{\Delta\Phi_2{}^{(1)}\} \tag{24}$$

$$\{\Psi_{2d}{}^{(1)}\}^p = \{\Psi_{2d}{}^{(1)}\} + \{\Delta\Psi_{2d}{}^{(1)}\}. \tag{25}$$

The expressions for the deviation matrices in (22)–(25) are quite complicated and will be omitted here in order to conserve space. They can be found in [8]. However, it is important to note that the kith elements of the square deviation matrices in (22) and (23) and the kth elements of the column deviation matrices in (24) and (25) can each be expanded as the sum of two terms, both being proportional to the deviation in element length. For example, the kith element of the deviation matrix $[\Delta\Phi^{(m)}]$ in (22) can be written as

$$[\Delta\Phi^{(m)}]_{ki} = (\beta_0\Delta h_k)\,\Delta\Phi_{ki}{}^{(m)\prime} + (\beta_0\Delta h_i)\,\Delta\Phi_{ki}{}^{(m)\prime\prime} \tag{26}$$

where $\Delta\Phi_{ki}{}^{(m)\prime}$ and $\Delta\Phi_{ki}{}^{(m)\prime\prime}$ can be evaluated from integrals containing $S_i{}^{(m)}(z)$ and other functions [8]. Also

$$A_2{}^{(1)p} = A_2{}^{(1)} + (\beta_0\Delta h_2)\,\Delta A_2{}^{(1)} \tag{27}$$

$$\{A^{(2)}\}^p = \{A^{(2)}\} + \{\Delta A^{(2)}\} \tag{28}$$

$$\{A^{(3)}\}^p = \{A^{(3)}\} + \{\Delta A^{(3)}\} \tag{29}$$

where the current deviation coefficients $\Delta A_2{}^{(1)}$, $\{\Delta A^{(2)}\}$, and $\{\Delta A^{(3)}\}$ are to be determined.

In addition, the number $\Psi_{22d}{}^{(1)}$ appearing in the denominator of (11) will also be changed by length perturbation to $\Psi_{22d}{}^{(1)p}$:

$$\Psi_{22d}{}^{(1)p} = \Psi_{22d}{}^{(1)} + (\beta_0\Delta h_2)\,\Delta\Psi_{22d}{}^{(1)}. \tag{30}$$

Substituting (14)–(20) in (1) and (11)–(13), and noting (21)–(30), we obtain, after second-order deviation terms have been neglected,

$$\Delta A_2{}^{(1)} = \left[-\frac{\Delta\Psi_{22d}{}^{(1)}}{\Psi_{22d}{}^{(1)}} + \tan\beta_0 h_2\right] A_2{}^{(1)} \tag{31}$$

and

$$[\Phi^{(2)}]\{\Delta A^{(2)}\} + [\Phi^{(3)}]\{\Delta A^{(3)}\} = -[\Delta\Phi^{(2)}]\{A^{(2)}\} - [\Delta\Phi^{(3)}]\{A^{(3)}\} - \{\Delta\Phi_2{}^{(1)}\}A_2{}^{(1)} - \{\Phi_2{}^{(1)}\}(\beta_0 h_2)\,\Delta A_2{}^{(1)} \tag{32}$$

and

$$[\Psi_d{}^{(2)}]\{\Delta A^{(2)}\} + [\Psi_d{}^{(3)}]\{\Delta A^{(3)}\} = -[\Delta\Psi_d{}^{(2)}]\{A^{(2)}\} - [\Delta\Psi_d{}^{(3)}]\{A^{(3)}\} - \{\Delta\Psi_{2d}{}^{(1)}\}A_2{}^{(1)} - \{\Psi_{2d}{}^{(1)}\}(\beta_0\Delta h_2)\,\Delta A_2{}^{(1)}. \tag{33}$$

In view of (26) and the attendant remarks, as well as of (30), the kth element of the right side of (32) can be written as

$$\sum_{i=1}^{N} [P_2]_{ki}\Delta h_i$$

where $[P_2]$ is an $N \times N$ square matrix. Similarly, another $N \times N$ matrix $[P_3]$ can be defined from the right side of (33). Equations (32) and (33) become

$$\begin{bmatrix} [\Phi^{(2)}] & [\Phi^{(3)}] \\ [\Psi_d{}^{(2)}] & [\Psi_d{}^{(3)}] \end{bmatrix} \begin{Bmatrix} \{\Delta A^{(2)}\} \\ \{\Delta A^{(3)}\} \end{Bmatrix} = \begin{bmatrix} [P_2] \\ [P_3] \end{bmatrix} \{\Delta h\}. \tag{34}$$

From (34), $\{A^{(2)}\}$ and $\{A^{(3)}\}$ can be found by matrix inversion:

$$\begin{Bmatrix} \{\Delta A^{(2)}\} \\ \{\Delta A^{(3)}\} \end{Bmatrix} = \begin{bmatrix} [\Phi^{(2)}] & [\Phi^{(3)}] \\ [\Psi_d{}^{(2)}] & [\Psi_d{}^{(3)}] \end{bmatrix}^{-1} \begin{bmatrix} [P_2] \\ [P_3] \end{bmatrix} \{\Delta h\} = \begin{bmatrix} [Q_2] \\ [Q_3] \end{bmatrix} \{\Delta h\}. \tag{35}$$

The perturbed current coefficients $\{A^{(2)}\}^p$ and $\{A^{(3)}\}^p$ can then be determined from (27)–(29). We note that the development parallels closely to that for spacing perturbation [1], although, of course, the elements of the various matrices involved are different.

IV. RADIATION FIELD FROM PERTURBED ARRAY

The radiation field of a length-perturbed Yagi–Uda array at a distance R_0 from a reference origin is

$$E'(\theta,\phi) = \frac{j\omega\mu_0}{4\pi R_0}\sum_{i=1}^{N} \exp(j\beta_0 d_i \sin\theta\cos\phi) \cdot \int_{-(h_i+\Delta h_i)}^{h_i+\Delta h_i} I_i^p(z_i') \exp(j\beta_0 z_i'\cos\theta)\sin\theta\,dz_i'. \tag{36}$$

Using (14)–(21), we can express $E'(\theta,\phi)$ as the sum of the radiation field $E(\theta,\phi)$ of the unperturbed array and a perturbation field:

$$E'(\theta,\phi) = E(\theta,\phi) + \frac{j\omega\mu}{4\pi R_0}\sum_{i=1}^{N} \exp(j\beta_0 d_i\sin\theta\cos\phi) \cdot \int_{-h_i}^{h_i} \sum_{m=1}^{3} [\Delta A_i{}^{(m)} S_i{}^{(m)}(z_i') + (\beta_0\Delta h_i) A_i{}^{(m)}\Delta S_i{}^{(m)}(z_i')] \exp(j\beta_0 z_i'\cos\theta) \cdot \sin\theta\,dz_i'. \tag{37}$$

It is convenient to define the following quantities for the integrals in (37):

$$M_2^{(1)}(\theta) = \frac{\beta_0}{2}\int_{-h_2}^{h_2} S_2^{(1)}(z_i')\exp(j\beta_0 z_i'\cos\theta)\sin\theta\, dz_i' \tag{38}$$

$$M_i^{(2)}(\theta) = \frac{\beta_0}{2}\int_{-h_i}^{h_i} S_i^{(2)}(z_i')\exp(j\beta_0 z_i'\cos\theta)\sin\theta\, dz_i' \tag{39}$$

$$M_i^{(3)}(\theta) = \frac{\beta_0}{2}\int_{-h_i}^{h_i} S_i^{(3)}(z_i')\exp(j\beta_0 z_i'\cos\theta)\sin\theta\, dz_i' \tag{40}$$

$$M_i^{(4)}(\theta) = \frac{\beta_0}{2}\int_{-h_i}^{h_i} \Delta S_i^{(1)}(z_i')\exp(j\beta_0 z_i'\cos\theta)\sin\theta\, dz_i'. \tag{41}$$

Substitution of (35) and (38)–(41) in (37) enables us to write

$$\begin{aligned} E'(\theta,\phi) &= E(\theta,\phi) + \Delta E(\theta,\phi) \\ &= E(\theta,\phi) + \{D\}^T\{\Delta h\} \end{aligned} \tag{42}$$

where the superscript T denotes transposition, and $\{D\}$ is an $N \times 1$ column matrix whose kth element is

$$\begin{aligned} D_k = \frac{j60}{R_0}\{&[A_k^{(2)}\sin\beta_0 h_k + \tfrac{1}{2}A_k^{(3)}\sin\tfrac{1}{2}\beta_0 h_k]\tan\theta \\ &\cdot\sin(\beta h_k\cos\theta)\exp(j\beta_0 d_k\sin\theta\cos\phi) \\ &+ \sum_{j=1}^{N}([Q_2]_{jk}M_j^{(2)}(\theta) + [Q_3]_{jk}M_j^{(3)}(\theta)) \\ &\cdot\exp(j\beta_0 d_j\sin\theta\cos\phi)\}, \qquad k \neq 2. \end{aligned} \tag{43}$$

For $k = 2$,

$$\begin{aligned} D_2 = \frac{j60}{R_0}\{&[A_2^{(1)}M_2^{(4)}(\theta) + \Delta A_2^{(1)}M_2^{(1)}(\theta)] \\ &\cdot\exp(j\beta_0 d_2\sin\theta\cos\phi) + [A_2^{(2)}\sin\beta_0 h_2 \\ &+ \tfrac{1}{2}A_2^{(3)}\sin\tfrac{1}{2}\beta_0 h_2]\tan\theta\sin(\beta_0 h_2\cos\theta)\exp(j\beta_0 d_2 \\ &\cdot\sin\theta\cos\phi) + \sum_{j=1}^{N}([Q_2]_{j2}M_j^{(2)}(\theta) + [Q_3]_{j2}M_j^{(3)}(\theta)) \\ &\cdot\exp(j\beta_0 d_j\sin\theta\cos\phi)\} \end{aligned} \tag{44}$$

where $[Q_2]_{jk}$ and $[Q_3]_{jk}$ denote, respectively, the jkth element of the square matrices $[Q_2]$ and $[Q_3]$ defined in (35). Equation (42), which expresses the deviation field ΔE explicitly in terms of length perturbations $\{\Delta h\}$, enables us to formulate a directivity-optimization procedure by adjusting the lengths of the array elements.

V. DIRECTIVITY OPTIMIZATION BY LENGTH PERTURBATION

To increase the directivity of a Yagi–Uda array by length perturbation, we follow a procedure similar to that used for spacing perturbation [1]. The directivity of an array in the direction (θ_0,ϕ_0) is

$$G(\theta_0,\phi_0) = \frac{|E(\theta_0,\phi_0)|^2}{60P_{\text{in}}} \tag{45}$$

where P_{in} is the time-average input power. With length perturbation E becomes E', P_{in} becomes P_{in}', and the perturbed directivity becomes

$$G'(\theta_0,\phi_0) = \frac{|E'(\theta_0,\phi_0)|^2}{60P_{\text{in}}'}. \tag{46}$$

From (42)

$$|E'(\theta_0,\phi_0)|^2 = |E|^2 + 2\{\Delta h\}^T\{B_1\} + \{\Delta h\}^T[\text{Re}\, C_1]\{\Delta h\} \tag{47}$$

where

$$\{B_1\} = \text{Re}\,(E\{D^*\}) \tag{48}$$

and

$$[\text{Re}\, C_1] = \text{Re}\,(\{D\}^*\{D\}^T). \tag{49}$$

P_{in}' in (46) is

$$P_{\text{in}}' = \tfrac{1}{2}\,\text{Re}\,[V_{02}{}^*I_2{}^p(0)] = P_{\text{in}} + \{\Delta h\}^T\{B_2\} \tag{50}$$

where

$$P_{\text{in}} = \tfrac{1}{2}V_{02}\,\text{Re}\,\{\sum_{m=1}^{3} A_2^{(m)}S_2^{(m)}(0)\}. \tag{51}$$

The kth element of $\{B_2\}$ in (50) is

$$\{B_2\}_k = \begin{cases} \tfrac{1}{2}V_{02}\,\text{Re}\,\{[Q_2]_{2k}S_2^{(2)}(0) + [Q_3]_{2k}S_2^{(3)}(0)\}, \\ \qquad\qquad k \neq 2 \\ \tfrac{1}{2}V_{02}\,\text{Re}\,\{[Q_2]_{22}S_2^{(2)}(0) + [Q_3]_{22}S_2^{(3)}(0) \\ \quad + \Delta A_2^{(1)}S_2^{(1)}(0) + A_2^{(1)}\Delta S_2^{(1)}(0) \\ \quad + A_2^{(2)}\Delta S_2^{(2)}(0) + A_2^{(3)}\Delta S_2^{(3)}(0)\}, \qquad k = 2. \end{cases} \tag{52}$$

For a lossless array, P_{in}' can be written in an alternative form [1]

$$P_{in}' = P_{in} + 2\{\Delta h\}^T\{B_3\} + \{\Delta h\}^T[\mathrm{Re}\, C_2]\{\Delta h\} \quad (53)$$

where

$$P_{in} = \frac{1}{240\pi}\int_0^{2\pi} d\phi \int_0^{\pi} |E(\theta,\phi)|^2 \sin\theta\, d\theta\, d\phi \quad (54)$$

$$\{B_3\} = \frac{1}{240\pi}\int_0^{2\pi} d\phi \int_0^{\pi} \{B_1\} \sin\theta\, d\theta\, d\phi \quad (55)$$

and

$$[C_2] = \frac{1}{240\pi}\int_0^{2\pi} d\phi \int_0^{\pi} [C_1] \sin\theta\, d\theta\, d\phi. \quad (56)$$

$\{B_1\}$ and $[C_1]$ in (55) and (56) have been defined in (48) and (49), respectively, and $[C_2]$ is a positive definite Hermitian matrix.

The change in directivity due to length perturbation $\{\Delta h\}$ is

$$\Delta G(\theta_0,\phi_0) = G'(\theta_0,\phi_0) - G(\theta_0,\phi_0) \quad (57)$$

which, by the use of (45)–(53), becomes

$$\Delta G(\theta_0,\phi_0) = \frac{1}{60}\frac{\{\Delta h\}^T\{B\} + \{\Delta h\}^T[\mathrm{Re}\, C_1]\{\Delta h\}}{P_{in} + 2\{\Delta h\}^T\{B_3\} + \{\Delta h\}^T[\mathrm{Re}\, C_2]\{\Delta h\}} \quad (58)$$

where

$$\{B\} = 2\{B_1\} - 60G(\theta_0,\phi_0)\{B_2\}. \quad (59)$$

We note that the negative sign in (59) for $\{B\}$ in the numerator of $\Delta G(\theta_0,\phi_0)$ in (58) indicates that the array directivity may decrease for an improper choice of $\{\Delta h\}$.

In order to be certain that $\Delta G(\theta_0,\phi_0)$ will be positive, we make use of a known relation in the theory of matrices [1], [2], which asserts that if the length changes in $\{\Delta h\}$ are chosen such that

$$\{\Delta h\} = \alpha[\mathrm{Re}\, C_2]^{-1}(2\{B_1\} - 60G\{B_2\}) \quad (60)$$

then

$$\Delta G = \frac{1}{60}\frac{\alpha(2\{B_1\} - 60G\{B_2\})^T[\mathrm{Re}\, C_2]^{-1}(2\{B_1\} - 60G\{B_2\}) + \{\Delta h\}^T[\mathrm{Re}\, C_1]\{\Delta h\}}{P_{in} + 2\{\Delta h\}^T\{B_3\} + \{\Delta h\}^T[\mathrm{Re}\, C_2]\{\Delta h\}} > 0. \quad (61)$$

The α in (60) should be sufficiently small to satisfy the condition $(\Delta h_i)/h_i \ll 1$. The new directivity G' as the result of length changes specified by (60) can be calculated from (61) and (57). A second perturbation can then be performed on G', and the process repeated until further increases are negligible. Again similar to the spacing perturbation procedure, the iterative process converges rapidly.

By combining the spacing and length perturbation procedures, we can obtain a Yagi–Uda array of dipole elements of optimum lengths that are optimally spaced to yield a maximum possible directivity. The elements will in general be nonuniformly spaced and their lengths will be different. Typical results will be illustrated by numerical examples in the following section.

VI. NUMERICAL EXAMPLES

We present here the computed results of two examples that illustrate the effectiveness of the length-perturbation procedure for increasing the directivity of a Yagi–Uda array. In both cases we start with a six-element array that consists of a driven dipole, a reflector, and four uniformly spaced directors of equal lengths. The reflector is situated a quarter-wavelength behind the driven element, as this combination has been found to be optimum relative to directivity [1], [4], [6]. Length perturbation (keeping the spacings fixed) is applied to the array in the first example to maximize the directivity. In the second example, a double-perturbation procedure is used, in which the element spacings and then the element lengths are adjusted in order to obtain a maximum directivity.

Example 1

Six-Element Yagi–Uda Array: Reflector length, $2h_1 = 0.510\lambda$; driver length, $2h_2 = 0.490\lambda$; equal length of four directors, $2h_3 = 2h_4 = 2h_5 = 2h_6 = 0.430\lambda$; dipole radius, $a = 0.003369\lambda$; element spacings $b_{21} = 0.250\lambda$, $b_{32} = b_{43} = b_{54} = b_{65} = 0.310\lambda$. The lengths of all the elements are to be adjusted for a maximum directivity.

The directivity of the initial array referring to that of a half-wave dipole is calculated by using (11)–(13), (45), and (51) to be 7.544(8.77 dB). Now keeping the element spacings fixed, the lengths of all the dipole elements are perturbed in accordance with (60). Three iterations converge rapidly to a directivity (referring to a half-wave dipole) of 10.012 (10 dB), an increase of 32 percent from the initial array. The new lengths of the six elements in the perturbed array are given in Table I. Several length combinations obtained by Green [5] for optimum six-element uniform Yagi–Uda arrays (all directors of equal lengths) on the basis of sinusoidal current distributions have been recomputed using the three-term approximation. In comparison, the directivity of the six-element length-perturbed array is more than 15 percent higher than that computed from Green's data.

The normalized radiation patterns for both the initial and the optimized arrays are given in Fig. 2. It is seen that the pattern for the optimized array has a slightly narrower main beam and lower sidelobes.

Example 2

Six-Element Yagi–Uda Array: Reflector length, $2h_1 = 0.510\lambda$; driver length, $2h_2 = 0.490\lambda$; equal length of four directors, $2h_3 = 2h_4 = 2h_5 = 2h_6 = 0.430\lambda$; dipole radius,

TABLE I
DIRECTIVITY OPTIMIZATION FOR SIX-ELEMENT YAGI–UDA ARRAY (PERTURBATION OF ELEMENT LENGTHS)

	h_1/λ	h_2/λ	h_3/λ	h_4/λ	h_5/λ	h_6/λ	Directivity (referring to half-wave dipole)
Initial Array	0.255	0.245	0.215	0.215	0.215	0.215	7.544
Length-Perturbed Array	0.236	0.228	0.219	0.222	0.216	0.202	10.012

$b_{21} = 0.250\lambda$, $b_{i2} = 0.310\lambda (i = 3,4,5,6)$, $a = 0.003369\lambda$.

TABLE II
DIRECTIVITY OPTIMIZATION FOR SIX-ELEMENT YAGI-UDA ARRAY (PERTURBATION OF ELEMENT SPACINGS AND ELEMENT LENGTHS)

	h_1/λ	h_2/λ	h_3/λ	h_4/λ	h_5/λ	h_6/λ	b_{21}/λ	b_{32}/λ	b_{43}/λ	b_{54}/λ	b_{65}/λ	Directivity (referring to half-wave dipole)
Initial Array	0.255	0.245	0.215	0.215	0.215	0.215	0.250	0.310	0.310	0.310	0.310	7.544
Array after Spacing Perturbation			Same as above				0.250	0.289	0.406	0.323	0.422	11.687
Optimum Array after Spacing and Length Perturbations	0.238	0.226	0.218	0.215	0.217	0.215			Same as above			13.356

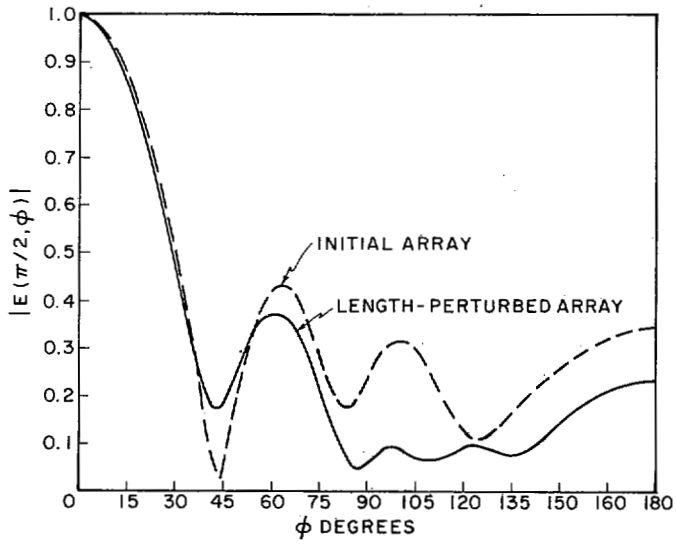

Fig. 2. Normalized patterns of six-element Yagi–Uda arrays (Example 1).

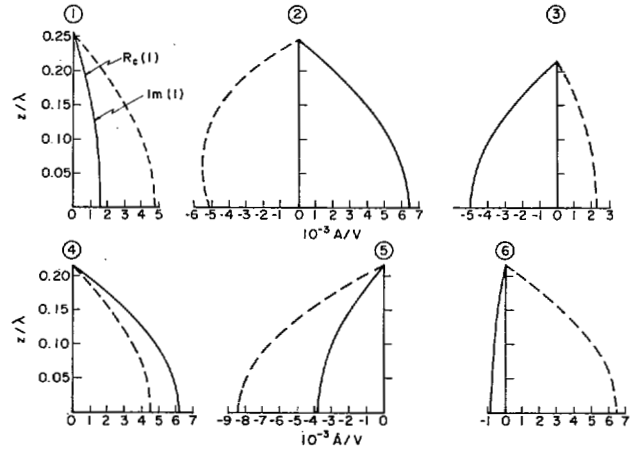

Fig. 3. Currents in initial six-element Yagi–Uda array with uniformly spaced directors of equal length. —— Re (I). —— Im (I).

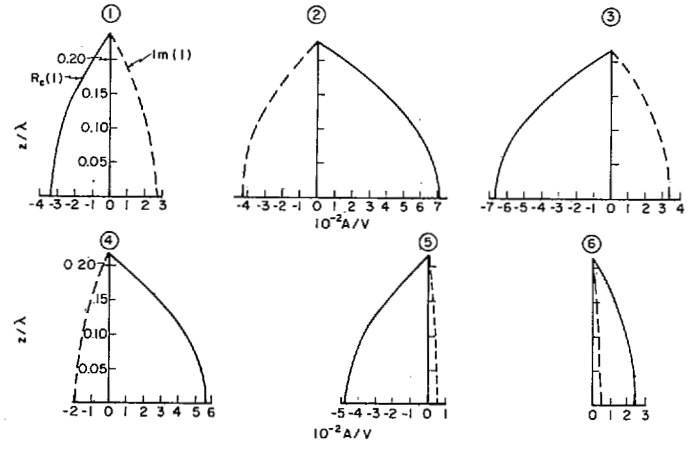

Fig. 4. Currents in optimum six-element Yagi–Uda array after spacing and length perturbations (Example 2). —— Re (I). —— Im (I).

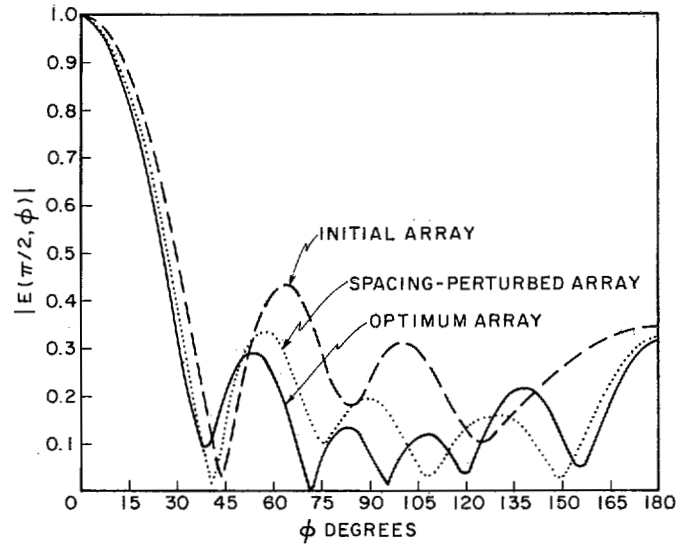

Fig. 5. Normalized patterns of six-element Yagi–Uda arrays (Example 2).

$a = 0.003369\lambda$; element spacings $b_{21} = 0.250\lambda$, $b_{32} = b_{43} = b_{54} = b_{65} = 0.310\lambda$. A double-perturbation procedure is to be applied, spacing perturbation followed by length perturbation, in order to obtain the maximum possible directivity.

This array is initially the same as the one given in Example 1. We first keep the lengths of the array elements fixed and apply the spacing-perturbation technique [1] to obtain the proper element spacings for maximum directivity. Only one iteration is needed to increase the directivity referring to a half-wave dipole from 7.544 (8.77 dB) to 11.687 (10.68 dB), an increase of 55 percent. With the new spacings we adjust the lengths of the dipoles in accordance with the procedure developed in the preceding section to increase the directivity further. After three iterations we obtain the data listed in the last line of Table II. The directivity referring to that of a half-wave dipole is now 13.356 (11.25 dB), an increase of 77 percent from that of the initial array. As shown in Table II, the array elements are now nonuniformly spaced and are of different lengths. It is found that a further application of the double-perturbation process does not yield a significant improvement.

The real and imaginary parts of the currents in the six elements of the initial array are plotted in Fig. 3, and those for the optimized array in Fig. 4. The absolute current amplitudes in the elements of the optimized array after spacing and length perturbations are about ten times those in the initial array. The input admittance for the optimum array in Table II is found to be $0.07136 - j0.04293$, while that for the initial array is $0.006503 - j0.005135$. The computed field intensity in the direction of maximum radiation for the initial array is only one-nineteenth of that for the optimized array.

The normalized radiation patterns for the initial array, the array after spacing perturbation, and the optimum array after both spacing and length perturbations are plotted in Fig. 5. We see that higher directivity is accompanied by a slightly narrower main beam, lower sidelobes, and a higher front-to-back ratio. These results may be explained by a comparison of the current amplitudes and phases in the array elements 2 through 6 before and after optimization, as follows.[1]

	$I_2 \angle \theta_2$	$I_3 \angle \theta_3$	$I_4 \angle \theta_4$	$I_5 \angle \theta_5$	$I_6 \angle \theta_6$
Uniform:	$8.2 \angle -39°$	$5.5 \angle -205°$	$7.7 \angle -324°$	$9.2 \angle -475°$	$6.6 \angle -612°$
Optimized:	$8.2 \angle -31°$	$7.5 \angle -207°$	$6.0 \angle -380°$	$4.8 \angle -547°$	$2.5 \angle -708°$
	$\theta_2 - \theta_3$	$\theta_3 - \theta_4$	$\theta_4 - \theta_5$	$\theta_5 - \theta_6$	
Uniform:	166°	119°	151°	137°	
Optimized:	176°	173°	167°	161°	

We note that the amplitudes and phases in the uniform array fluctuate widely, whereas in the optimized array the amplitudes decrease smoothly and rapidly and the phases decreasc continuously and slowly. The optimization procedure with respect to element spacings and element lengths apparently leads to an array on which a predominantly traveling wave is sustained. Hence an increased directivity is accompanied by a generally improved radiation pattern.

[1] The authors are indebted to the reviewer who supplied them with this analysis.

VII. CONCLUDING REMARKS

Employing a perturbation technique, a method has been developed for the maximization of the directivity of a Yagi–Uda array by adjusting the lengths of the dipole elements. The effects of a finite element radius and the mutual coupling between the elements are taken into consideration. A three-term expansion with complex coefficients is used to approximate the current distribution in the dipoles and to convert the governing integral equations into matrix equations. The method is systematic and rapidly convergent, and it yields the optimum lengths of all elements simultaneously. The length-perturbed array is guaranteed to have an increased directivity and no trial-and-error process is involved.

By combining the length-perturbation procedure with the spacing-perturbation procedure developed in a previous paper [1], a Yagi–Uda array with dipole elements of optimum lengths and optimum spacings is obtained which has a max–max directivity. Typical results for a doubly perturbed six-element optimum array show a tenfold increase in current amplitudes in the dipole elements and a generally improved radiation pattern.

As in most multiparameter synthesis and optimization problems, the solution is not unique. There are many minor maxima for directivity in the multidimensional space. Hence the initial choice is expected to affect the end result as well as the rate of convergence; so is the order of double perturbation. It is wise to start with an initial array that is known to have a good directivity either from empirical data or from experimentation.

REFERENCES

[1] D. K. Cheng and C. A. Chen, "Optimum element spacings for Yagi–Uda arrays," *IEEE Trans. Antennas Propagat.*, vol. AP-21, pp. 615–623, Sept. 1973.
[2] F. I. Tseng and D. K. Cheng, "Spacing perturbation techniques for array optimization," *Radio Sci.*, vol. 3 (New Series), pp. 451–457, May 1968.
[3] D. K. Cheng, "Optimization techniques for antenna arrays," *Proc. IEEE*, vol. 59, pp. 1664–1674, Dec. 1971.
[4] H. W. Ehrenspeck and H. Poehler, "A new method for obtaining maximum gain from Yagi antennas," *IRE Trans. Antennas Propagat.*, vol. AP-7, pp. 379–386, Oct. 1959.

[5] H. E. Green, "Design data for short and medium length Yagi–Uda arrays," *Elec. Eng. Trans.* (Australia), paper 2037, pp. 1–8, Mar. 1966.
[6] R. W. P. King, R. B. Mack, and S. S. Sandler, *Arrays of Cylindrical Dipoles.* New York: Cambridge, 1968.
[7] D. K. Cheng and C. A. Chen, "Optimum element spacings for Yagi–Uda arrays," Syracuse University, Syracuse, N. Y., Tech. Rep. TR-72-9, Nov. 1972.
[8] C. A. Chen, "Perturbation techniques for directivity optimization of Yagi–Uda arrays," Ph.D. dissertation, Syracuse University, Syracuse, N. Y., 1974.

Ferroscan: Toward Continuous-Aperture Scanning

ERNEST STERN, SENIOR MEMBER, IEEE, AND G. N. TSANDOULAS, MEMBER, IEEE

Abstract—**Work done several years ago, which represents a step toward eliminating the necessity for subdividing a phased array aperture into many discrete elements, each with its own phase shifter, is reported on for the first time. A 5-wavelength, *X* band horn aperture, partially loaded with ferrite material, was designed and fabricated. The resulting antenna replaces at least 10 conventional phase shifter-element units and was successfully controlled by an external magnetic circuit to form sum and difference patterns and to scan the beam.**

INTRODUCTION

THE RESEARCH and development accorded to the phased array in the last decade was principally due to requirements for increased radar versatility. Phased array antennas have become progressively more sophisticated instruments that provide rapid and reliable electronic scanning capability as well as certain signal processing functions at the radar "front end."

The operation of differential shifting of the phase of the radiated wave, essential to beam scanning, has been traditionally carried out by dividing the antenna aperture into many individual radiating elements and attaching to each of these an electronically controlled phase shifting device. This process of aperture discretization has worked reasonably well but at considerable cost and great complexity, the very things that many consider to be the Achilles' heel of phased arrays. One answer to these drawbacks is component integration in which one component performs several functions. For example, a radiating element, which is its own phase shifter, would be in this category. Another example is the use of continuous-aperture scanning. In continuous-aperture scanning the aperture is used in its original unbroken form and a progressive phase change is applied across the aperture without subdividing it into separate elements.

In this work, we are focusing attention on continuous-aperture scanning with a technique that we call Ferroscan. In our example, we replace at least 10 discrete phase shifter-element units with a single ferrite-loaded aperture whose properties are externally controlled to scan a beam.

Manuscript received May 9, 1974; revised August 13, 1974. This work was sponsored by the Department of the Army.
The authors are with Lincoln Laboratory, Massachusetts Institute of Technology, Lexington, Mass. 02173.

THE FERROSCAN PRINCIPLE

The Ferroscan idea consists of using ferrite, which partially fills an aperture, as a field displacement device. In Fig. 1 an aperture of length L and width a is shown partially filled with ferrite material of thickness d. The remaining volume is occupied by a dielectric of relative dielectric constant ϵ_d. For an incident field with transverse (along x) variation only, such as the TE_{10} mode of a rectangular waveguide, a displacement of the field toward the more densely loaded portion of the aperture takes place, qualitatively shown in Fig. 1. The phenomenon is well known and has been described in the literature [1]. Such devices ordinarily involve waveguides whose cross sectional dimensions are less than 1/2 wavelength. The novel features of the ferrite loaded radiating section are that it is much wider than 1/2 wavelength and that the ferrite, which is operated in the remanent state, is magnetized in a step-wise fashion along its length by an external driver circuit. This can be used to generate a tilted phase front across the aperture and the outgoing wave may be scanned in the yz plane.

Taking the applied magnetic field to be in the y direction, the permeability tensor for remanent ferrite may be written as

$$\bar{\bar{\mu}} = \mu_0 \begin{bmatrix} \mu_r & 0 & j\kappa \\ 0 & 1 & 0 \\ -j\kappa & 0 & \mu_r \end{bmatrix}. \tag{1}$$

We characterize the remanent state [2] with the usual Polder expressions for μ_r and κ, with the internal magnetizing field set equal to zero. In this case, $\mu_r = 1$ and $\kappa = \omega_M/\omega$, where $\omega_M = \gamma\mu_0 M_r$. M_r is the remanent magnetization, and γ is the gyromagnetic ratio. These assumptions have yielded useful performance estimates for the rectan-